A Machine Learning Approach to Distribution Identification in Non-Gaussian Clutter

Justin Metcalf and Shannon Blunt
Electrical Eng. and Computer Sci. Dept.
University of Kansas

Braham Himed
Sensors Directorate
Air Force Research Laboratory

Abstract— **We consider a set of non-linear transformations of order statistics incorporated into a machine learning approach to perform distribution identification from data with low sample support with the ultimate goal of determining the appropriate detection threshold. The set of transformations provide a means with which data may be compared to a library of known clutter distributions. Several common non-Gaussian distributions are discussed and incorporated into the initial implementation of the library. This approach allows for the addition of empirically measured clutter distributions, which may not have a known analytic form. The adaptive threshold estimation reduces the probability of false alarm when non-Gaussian clutter is present..**

I. INTRODUCTION

At a fundamental level, the problem of radar detection is expressed as a statistical hypothesis test: does the sampled data correspond to a null distribution of clutter and noise or to the alternate, target-present distribution. Both the null and alternate distributions are dependent on the radar system under consideration, as well as the operating environment in which the radar will be expected to perform. By taking a machine learning approach, the flexibility and robustness of the radar may be enhanced so that it may successfully operate in unforeseen, adverse scenarios.

The succeeding layers of processing in a radar system (*e.g.* tracker, target identification) depend on reliable performance by the detector. To provide a reliable detection of targets, the detector must closely approximate the true statistical distribution of both hypotheses with a modeled distribution. If the true and alternate hypotheses are known, the Neyman-Pearson (NP) criterion may be applied to determine a threshold that maximizes the probability of detection while maintaining a desirable, constant rate of false alarm [1]. However, in practice the true distribution, as well as its parameters (*e.g.* shape, scale, variance) cannot be clairvoyantly known. At the very least, the mean and variance of the null distribution must be known to set the NP threshold optimally.

With the absence of *a priori* information about the clutter distribution, it is common to assume that the clutter is homogeneous and complex Gaussian distributed with an unknown covariance structure. An adaptive, sub-optimal detector can then be formed by using range cells near the cell-under-test (CUT) to estimate the clutter statistics and form a detection threshold. The well known Kelly generalized likelihood ratio test (GLRT) follows this logic [2]. As an alternative, the adaptive matched filter (AMF) has a lower computational cost when compared to the GLRT, but suffers a penalty in SNR [3]. However, the performance of both the GLRT and AMF depend on the assumption of homogenous, Gaussian data [4].

Non-Gaussian clutter distributions with heavier tails have long been observed in practice, most notably in measurements of sea clutter [5]. For a non-Gaussian distribution, additional parameters such as shape and scale must also be estimated from the data. Therefore, to establish a reliable detection threshold the true distribution of the clutter must be identified and any relevant parameters must be estimated. Previous work proposed a graphically-based approach to distribution identification [6], [7].

Here we extend the work of [6], [7] to a general machine learning framework for distribution, and ultimately threshold, estimation. Current radar signal processing research emphasizes the role of knowledge-aided and cognitive approaches to future radar systems. In a knowledge-aided approach, measured data can be leveraged to provide candidate models for radar clutter. However, the framework established here is open to future innovations which may allow the radar system to add to its knowledge base in a cognitive manner. In particular, it has been shown that measured data may fit two analytical distributions equally well [8]. This fact raises the question of the existence of an unknown distribution whose parameters may be inferred from known distributions. More importantly, the primary motivation of modeling the clutter with a statistical distribution is to maximize the accuracy of an estimated threshold via the NP criterion. Therefore, our true goal is to establish a robust, low complexity implementation of a radar clutter threshold estimator. In this implementation, a collection of threshold information may then be used to determine a proper threshold for detection in non-Gaussian clutter that may be distributed according to an unknown, empirically measured distribution. In this paper we describe the framework and provide an intuition to the overall strategy and illuminate the discussion with preliminary results.

II. MODELING RADAR CLUTTER

In general, it is difficult to predict the clutter characteristics that a radar might encounter in its operational life. Clutter characteristics depend on both radar parameters (*e.g.* range resolution, grazing angle, beamwidth) as well as the physical characteristics of the illuminated area (*e.g.* mountainous vs.

littoral regions). In particular, the likelihood of encountering "spiky" or heavy-tailed clutter increases as range resolution becomes finer and as grazing angle decreases [8]–[11]. The spiky nature of the clutter naturally leads to an increase in false alarms by the detector. A general characterization of a clutter process must be able to model both the amplitude statistics of a single pulse as well as the correlation between individual pulses [9], [12].

Clutter is often modeled as the backscattered radiation from a large number of random scatterers. Therefore, by the central limit theorem (CLT) the clutter is assumed to be Gaussian in nature [9]. However, if the number of scatterers can be expressed as a mixture of Poisson random variables, the clutter distribution takes the form of a spherically invariant random process (SIRP) [9], [13]. The theory of SIRPs allows the analysis and simulation of a class of multidimensional, correlated, non-Gaussian random vectors, denoted as spherically invariant random vectors (SIRVs). An individual SIRV is a conditionally Gaussian random vector that has been modulated by an instantiation of a positive random variable. Therefore a SIRV distributed clutter process is locally Gaussian, but the large scale sampling of the radar causes a power modulation to appear across an illuminated area. Many of the non-Gaussian distributions that have been empirically fit to measured clutter data belong to the class of SIRVs (*e.g.* the K distribution and the Weibull distribution for certain values of the shape parameter) [6], [7], [9], [13].

A length L complex SIRV $\mathbf{y}$ can be expressed in the quadratic form

$$q = \mathbf{y}^H \boldsymbol{\Sigma}^{-1} \mathbf{y} \tag{1}$$

where $(\bullet)^H$ denotes complex conjugate transpose and $\boldsymbol{\Sigma}$ is the covariance matrix of $\mathbf{y}$. Using (1), the pdf of $\mathbf{y}$ can be defined as

$$f_{\mathbf{Y}}(\mathbf{y}) = (\pi)^{-L} |\boldsymbol{\Sigma}|^{-1} \int_0^\infty v^{-2L} \exp\left(-\frac{q}{v^2}\right) f_V(v) \mathrm{d}v \tag{2}$$

where $|\boldsymbol{\Sigma}|$ is the determinant of the covariance matrix and V is the modulating random variable with pdf $f_V(v)$. It is straightforward to prove that the Gaussian distribution is a SIRV with $f_V(v) = \delta(v - 1)$ for $\delta(v)$ the delta function [7].

While not admissable as a SIRV [7], it has been suggested that the log-normal distribution is a good fit to measured clutter [14], [15]. Multivariate, correlated log-normal clutter may be generated by taking the complex exponential of zero mean, complex Gaussian random vectors [15].

A. Consequences of Non-Gaussian Clutter

To illustrate the consequences of non-Gaussian clutter, consider the increase in threshold required to maintain a constant false alarm rate in spiky clutter versus Gaussian clutter. Define the change in threshold to be

$$\Delta_{\mathrm{thresh}}(\mathrm{dB}) \doteq 10\log_{10}\left[\frac{\mathcal{T}_{\mathrm{NG}}}{\mathcal{T}_{\mathrm{G}}}\right] \tag{3}$$

where $\mathcal{T}_{\mathrm{NG}}$ is the threshold required to maintain a constant false alarm rate in a particular non-Gaussian distribution
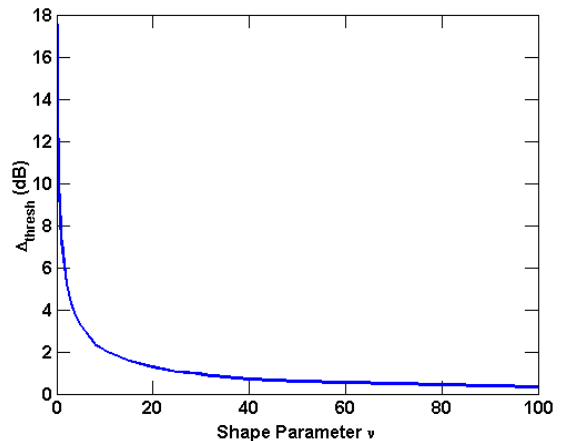

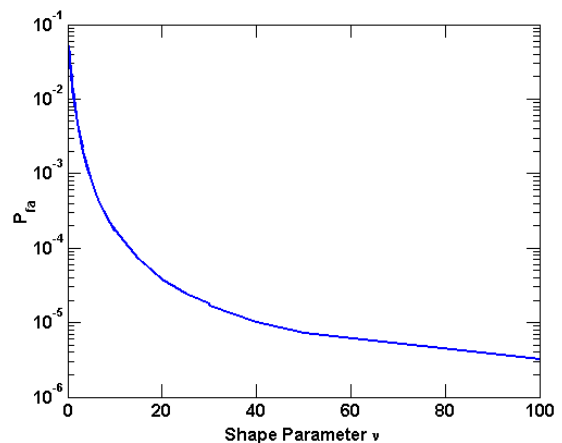Fig. 1. K distribution threshold v. shape parameter

Fig. 2. Increased P_{fa} from K distributed clutter

and $\mathcal{T}_{\mathrm{G}}$ is the threshold required to maintain an identical false alarm rate in complex Gaussian clutter. This change in threshold must be estimated, and directly corresponds to loss of detection probability. For K distributed clutter Figure 1 illustrates the increase in threshold for increasing shape parameter (note: the K distribution tends towards Gaussian as the shape parameter goes to infinity). Considered another way, if the detector uses a threshold derived from the Gaussian assumption but encounters heavy tailed clutter, the probability of false alarm will inevitably rise. Figure 2 shows the encountered probability of false alarm when a detector using $\mathcal{T}_{\mathrm{G}}$ is used in the presence of K distributed clutter with increasing shape parameter. For Figures 1 and 2, the desired probability of false alarm was set to $P_{\mathrm{fa}} = 10^{-6}$.

III. OZTURK ALGORITHM

We denote the algorithm presented in [6], [7], [16]–[18] as the Ozturk algorithm after its lead author. The goal of the Ozturk algorithm was to provide a graphical measure of distance between sampled data and the Gaussian distribution [16]–[18] using order statistics. The algorithm was then extended to provide a distance between various SIRV distributions and the

Gaussian distribution [7]. Through this extension, a library of candidate distributions can be formed. Here we describe the Ozturk algorithm in the context of arbitrary data (*i.e.* not necessarily in terms of radar clutter returns). We then show an example using SIRV distributed data and consider clutter returns in general in Section IV.

To provide a graphical distance between distributions, a set of vectors are formed from expected values of candidate distributions. These vectors are linked, and the endpoint of the linked vectors are plotted on a two dimensional plane, with coordinates (U, V). This process results in a unique endpoint for each candidate distribution in the library [7]. Sampled data may then be similarly transformed and compared to the endpoints in the library.

The nonlinear transformation of the Ozturk algorithm uses the studentized order statistics of candidate distributions. To begin, consider a collection of N complex independent, identically distributed (IID) data samples $\mathbf{q} = [q_1, q_2, \ldots, q_N]$. The sample mean and variance of $\mathbf{q}$ are denoted as $\bar{q}$ and $\hat{\sigma}^2$, respectively. The samples of $\mathbf{q}$ are then ordered, forming the order statistics

$$q_{(1)} \leq q_{(2)} \leq \cdots \leq q_{(N)}. \tag{4}$$

Finally, the studentized order statistics of $\mathbf{y}$ are defined as

$$z_{(i)} = \frac{q_{(i)} - \bar{q}}{\hat{\sigma}}. \tag{5}$$

Studentization allows for the order statistics to be normalized to zero mean and unit variance, to facilitate the comparison of sampled data from different distributions.

As mentioned above, the Ozturk algorithm is a two dimensional graphical approach. Therefore, the vectors may be represented by a magnitude and an angle. Let the angles ϕ_i be a uniform sampling of $(0, \pi)$, or

$$\phi_i = \pi \frac{i}{N+1}, \quad i = 1, \ldots, N. \tag{6}$$

The magnitude of each vector is given by $|z_{(i)}|$, and the angle with respect to the V axis is ϕ_i. Starting at $(0,0)$, the coordinates of the endpoint of each vector is then given as

$$U_k = \frac{1}{k} \sum_{i=1}^{k} \cos(\phi_i) |z_{(i)}|$$

$$V_k = \frac{1}{k} \sum_{i=1}^{k} \sin(\phi_i) |z_{(i)}|$$

$$k = 1, \ldots, N. \tag{7}$$

The endpoint (U_N, V_N) for each distribution in the library is then plotted.

Note that the number of data samples considered must be pre-determined when forming the library. However, the library may be created offline via Monte Carlo simulation for commonly expected data sizes. Further, observe that the Ozturk algorithm yields a hypothesis *suggestion* rather than an hypothesis test. In addition, the location of the endpoints are a function of the shape parameter of the data. Therefore,
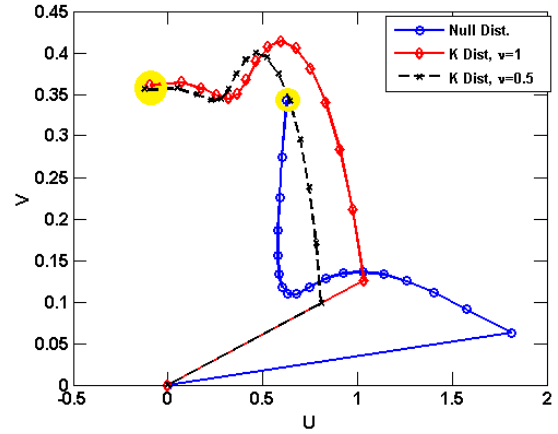

Fig. 3.   Example Ozturk Library, Linked Vectors (endpoints highlighted)

the Ozturk algorithm transforms sample data and returns both a distribution as well as a likely shape parameter.

As an example, Figure 3 shows a small library formed by three candidate distributions that have been transformed by the Ozturk algorithm. All three are length $L = 16$ SIRVs, that have been collapsed into the quadratic form given by (1). To generate Figure 3, 100,000 collections of $N = 16$ quadratic data samples were formed via Monte Carlo. The endpoints were then plotted for the complex Gaussian distribution as well as K distributions with shape parameters $\nu = 0.5$ and 1. Figure 3 illustrates the separation between the expected endpoints (yellow circles) associated with Gaussian distributed data and the heavier tailed K distribution.

A. Extension of the Ozturk Algorithm

The original intuition of the Ozturk algorithm was based on a graphical distance in a two dimensional plane. This formulation naturally led to the use of the sine and cosine functions to weight the magnitudes given by the order statistics of the candidate distributions. However, notice that in general (7) is a weighted sum of magnitudes. When considered in this light, the choice of sine and cosine functions become arbitrary.

Therefore, we propose the use of multiple weightings to provide further diversity. As a first approach, the aforementioned sine and cosine are included, along with their respective squares, the hyperbolic functions sinh, cosh, and tanh, and their squares. These additional weightings act to emphasize and de-emphasize different regions of the pdf of the sampled data. For example, when $\sin(\phi_i)$ is applied to the order statistics, the samples around the median are emphasized and the extreme values (maximum and minimum) are de-emphasized. Alternatively, the squared cosine emphasizes the extremes of a sample data set (minimum and maximum), while excising the median value from the sum. Note that by using the quadratic form of a SIRV in (1), the Ozturk algorithm is in essence performing a weighted summation of the order statistics of the generalized inner product (GIP) of sample data [19]. Thus, this extension can encompass multivariate non-Gaussian distributions which are not admissible as SIRVs (*e.g.*

log-normal distribution).

As a second extension, we propose the use of the Ozturk algorithm to directly estimate a threshold from sampled data. In other words, using the diversity of multiple weighting functions, we wish to provide a low complexity and low sample support method to directly infer a threshold to achieve a desired probability of false alarm from measured data. We refer to the combination of these two extensions as the extended Ozturk algorithm (EOA).

IV. LIBRARY IMPLEMENTATION

To test the new adaptive threshold estimation algorithm, a library is populated with a combination of weighting functions and candidate distributions. The individual elements of the receive vector are given by the returns from a single range cell over a coherent processing interval. Therefore, a collection of N range cells (assumed homogenous) is gathered with L complex returns per range cell (*i.e.* L pulses in a coherent processing interval). The distribution may then be described by the quadratic form of the SIRV, q, where the covariance matrix is estimated from the N vectors in the data sample. Note that the optimal estimation of the covariance matrix of SIRV data is not straightforward [20]. However, the use of studentized order statistics causes the Ozturk algorithm to be robust to scaling errors when estimating the covariance matrix [7].

The initial implementation of this library includes the classical K, Weibull, and log-normal distributions. Specifically, we consider collections of $N = 16$ length $L = 4$ complex random vectors. The Weibull distributed data was generated with shape parameters of $\nu = 0.1 - 2$, generated at increments of $\Delta \nu = 0.1$. The K distributed data was generated with a range of shape parameters $0.3 \leq \nu \leq 200$, with smaller sample increments at lower values of ν (*i.e.* where the clutter is "spikier" and the required threshold is much greater). For each distribution/shape parameter pair in the library, the optimal detection threshold has been computed via Monte Carlo, using 10^7 sample vectors for a $P_{fa} = 10^{-5}$. For the 10 weighting functions given in Section III-A, we performed 10^6 Monte Carlo simulations to find an average endpoint, providing a 10 dimensional space.

Figure 4 shows a cut from the 10 dimensional space using the sine and cosine weighting functions. Note that Figure 4 is equivalent to the original Ozturk algorithm, where studentized order statistics are weighted by the sine and cosine functions, and each resulting vector is summed to produce a two dimensional coordinate. The arcs plotted for each SIRV are parameterized by changing the shape parameter such that the distribution becomes increasingly heavy-tailed. Notice that each SIRV converges to the Gaussian distribution for a value of the shape parameter ν (*e.g.* $\nu \to \infty$ for the K distribution, $\nu \to 2$ for the Weibull distribution [7]). However, the log-normal distribution is not parametrized by a shape parameter, and therefore occupies a single point near the bottom center.
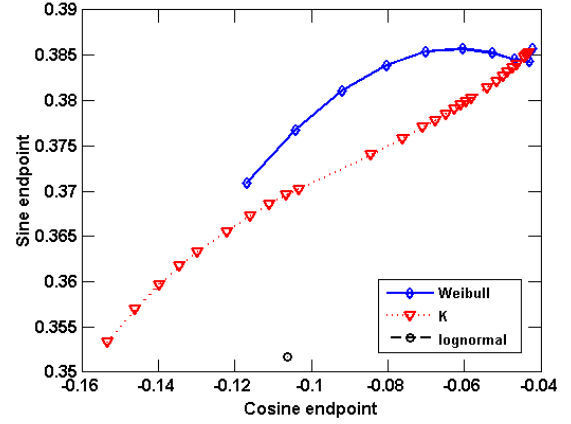

Fig. 4. Cosine v. sine average endpoints

V. SIMULATION RESULTS

The results in this section were generated via Monte Carlo with 10^5 runs per data point. As with the previous results, each data set consists of $N = 16$ length $L = 4$ complex vectors that are compressed into the quadratic, or GIP, form of (1). For this initial work, the true covariance matrix is used to form the GIP, as the Ozturk algorithm is robust to covariance matrix estimation error [7]. Future work will address the impact of using a sample covariance matrix.

A. Distribution Identification

Conventionally, to establish a detection threshold a modeled distribution must first be selected. Each sample data set is processed via equations (4)-(7), with different weighting functions substituted in (7) when indicated. For the K and Weibull distributions, the average endpoints in the library are linked linearly to form a piecewise linear curve. The sample end point is then compared to the two curves (for K and Weibull distributions) and the log-normal point. The closest curve (or point) is found and the corresponding distribution is chosen as the hypothesis suggestion as to which clutter distribution is present.

Figure 5 shows the rate at which the Weibull, K, and log-normal distributions are selected when sine and cosine weightings are used on K distributed data of varying shape parameters. Figure 6 shows the classification accuracy when the cosine and cosine squared weighting functions are used. Notice in both cases that the algorithm correctly selects the K distribution for very low shape parameters, but increasingly selects the Weibull distribution as the shape parameter increases (*i.e.* as the data tends towards Gaussian). In addition, the log-normal distribution is more likely to be chosen when the cosine and sine weightings are used as opposed to the cosine and cosine squared weightings. However, if distribution identification is desired so as to subsequently estimate the threshold, the direct determination of this threshold also bears consideration
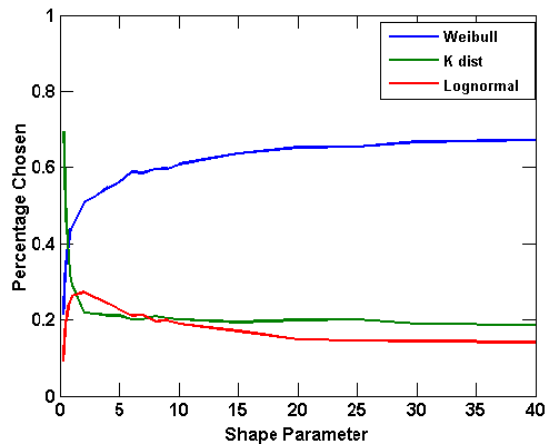
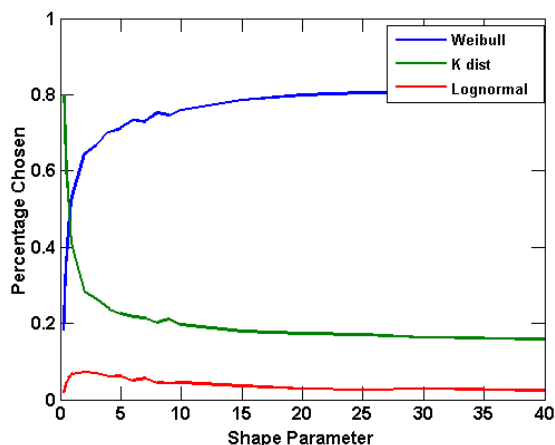Fig. 5. Classifying K data using cosine and sine weightings

Fig. 6. Classifying K data using cosine and cosine squared weightings

B. Threshold Estimation

In Section V-A it was shown that the Ozturk algorithm struggled with correctly classifying K distributed clutter for high shape parameters. However, the ultimate goal of a detector is to set an optimal threshold. In this section we investigate the capability of the EOA to determine a correct threshold, regardless of which distribution is selected. As the focus here is on a low computational complexity implementation, a lookup table/interpolation approach with desired $P_{fa} = 10^{-5}$ is employed. By finding the nearest point on the curve associated with a distribution, the shape parameter associated with a sample data point may be generated via linear interpolation between the two closest shape parameters that have known (*i.e.* pre-computed) thresholds. This process relies on adequate sampling by the library in regions where the shape parameter and threshold are related in a highly non-linear fashion, so that the behavior may be approximated in a piecewise linear fashion. To summarize the processing steps:

1) Collect a data set of N length L vectors (*i.e.* samples from N training range cells over a period of L pulses.)
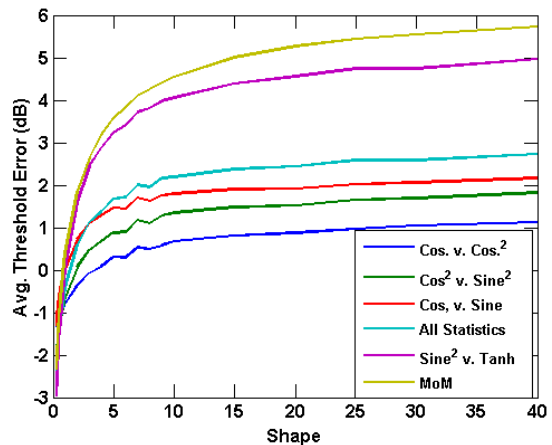2) Compress to a set of N GIPs via (1).

Fig. 7. Threshold estimation error - K distributed data

3) Sort and studentize the GIPs as (4) and (5).
4) Choose weighting functions and generate a sample endpoint from (6) and (7).
5) Find the closest point on a curve in the library.
6) Find the associated shape parameter via lookup or interpolation between the two nearest shape parameters that have known thresholds.
7) Find the corresponding threshold to the hypothesized distribution/shape parameter pair.

Note that with respect to the number of range cells used, the additional processing steps 3-4 increase linearly in complexity, and are unchanged with respect to the number of pulses. The remainder of the algorithm incurs a computational cost that depends on the size and sampling of the library, rather than the dimensionality of the data.

First, we examine the threshold estimation accuracy of the EOA on K distributed data. For comparison, the classical method of moments (MoM) estimator [21] is used to estimate the shape parameter of the data. Note that in this case the clairvoyant covariance matrix was also used, and the MoM has $L \times N = 48$ samples to estimate the shape parameter. The MoM estimated shape parameter was then translated into a threshold in the same way as the EOA estimated shape parameter, albeit with the K distribution always correctly selected. The average threshold estimated was then compared to the true threshold for varying shape parameters in decibel scale. The results for several pairs of weighting functions are shown in Figure 7.

Note that a threshold error above 0 dB produces an equal amount of detection loss, and any error below 0 dB corresponds to increasing P_{fa}. The selection of weighting functions appears to have a large amount of influence on the accuracy of the estimated threshold, especially at large values of ν. Recalling the behavior of Figure 1, an incorrect estimate of the shape parameter at high or low values causes a non-linearly related increase in error in the threshold estimate. However, the EOA selects a threshold corresponding to the data, and thereby produces an accurate result. Equation (7) can be extended to
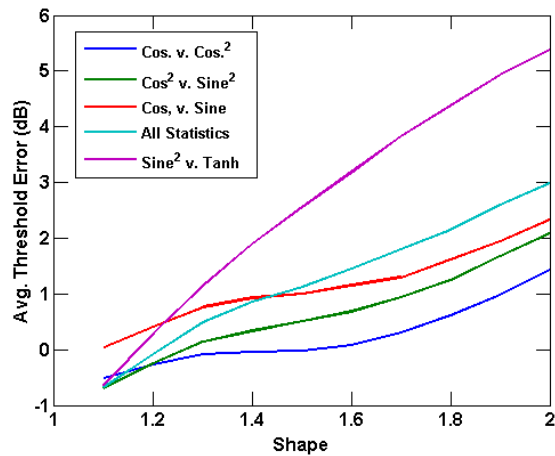
Fig. 8.   Threshold estimation error - Weibull distributed data

an arbitrary number of weighting functions, so we investigated the use of all 10 weighting functions under consideration to form an endpoint. That result is denoted as "All Statistics". Recall from Figures 5 and 6 that the cosine and cosine squared combination was less likely to select a log-normal distribution at high shape parameters than the sine and cosine weighting functions. For the parameters under consideration, the threshold for the log-normal distribution is 9.5 dB greater than the K distribution at $\nu = 40$, while it has approximately the same threshold for $\nu = 0.3$. Therefore, as the log-normal distribution has no degrees of freedom, it provides a strong bias to the average results when it is incorrectly selected for high shape parameter clutter.

In Figure 8, the use of the EOA is examined for threshold determination under Weibull distributed clutter. In this experiment, the EOA performs very well in Weibull clutter, capable of an average detection loss of ≈ 1 dB for $\nu = 2$, and a threshold within 1 dB for $\nu = 1.1$, which has a threshold 7.3 dB greater than the threshold required for complex Gaussian clutter of similar power.

VI. CONCLUSIONS

The approach shown here is an inherently sub-optimal approach to distribution identification. However, it is low complexity, robust, and amenable to expansion in the form of a cognitive radar. A true cognitive radar will have the capability to infer the distributional properties of a measured set of data from the entries in the distribution library. If enough deviation from previous known distributions is detected, a new distribution may be added to the library. The strategy presented here focuses on the desired result (a desired probability of false alarm) and allows the data to speak for itself (*i.e.* distribution agnostic) and selects the most appropriate threshold for the situation at hand.

ACKNOWLEDGMENT

REFERENCES

[1] M. A. Richards, J. A. Scheer, and W. Holm, *Principles of Modern Radar, Vol. I: Basic Principles*.   Scitech Publishing Inc., 2010.
[2] E. Kelly, "An adaptive detection algorithm," *Aerospace and Electronic Systems, IEEE Transactions on*, vol. AES-22, no. 2, pp. 115 –127, march 1986.
[3] F. Robey, D. Fuhrmann, E. Kelly, and R. Nitzberg, "A cfar adaptive matched filter detector," *Aerospace and Electronic Systems, IEEE Transactions on*, vol. 28, no. 1, pp. 208 –216, jan 1992.
[4] W. Melvin, "Space-time adaptive radar performance in heterogeneous clutter," *Aerospace and Electronic Systems, IEEE Transactions on*, vol. 36, no. 2, pp. 621 –633, apr 2000.
[5] G. Trunk, "Radar properties of non-rayleigh sea clutter," *Aerospace and Electronic Systems, IEEE Transactions on*, vol. AES-8, no. 2, pp. 196–204, 1972.
[6] M. Rangaswamy, D. Weiner, and A. Ozturk, "Non-gaussian random vector identification using spherically invariant random processes," *Aerospace and Electronic Systems, IEEE Transactions on*, vol. 29, no. 1, pp. 111 –124, jan 1993.
[7] M. Rangaswamy, P. Chakravarthi, D. Weiner, L. Cai, H. Wang, and A. Ozturk, "Signal detection in correlated gaussian and non-gaussian radar clutter," Rome Laboratory, Tech. Rep. 93-17391, 1993.
[8] E. Conte, A. De Maio, and C. Galdi, "Statistical analysis of real clutter at different range resolutions," *Aerospace and Electronic Systems, IEEE Transactions on*, vol. 40, no. 3, pp. 903 – 918, july 2004.
[9] K. Sangston and K. Gerlach, "Coherent detection of radar targets in a non-gaussian background," *Aerospace and Electronic Systems, IEEE Transactions on*, vol. 30, no. 2, pp. 330 –340, apr 1994.
[10] R. R. Boothe, "The weibull distribution applied to the ground clutter backscatter coefficient," U.S. Army Missile Command, Tech. Rep. RE-TR.69-15, june 1969.
[11] J. B. Billingsley, "Ground clutter measurements for surface-sited radar," Lincoln Laboratories, Tech. Rep. 786, 1993.
[12] A. Farina, A. Russo, F. Scannapieco, and S. Barbarossa, "Theory of radar detection in coherent weibull clutter," *Communications, Radar and Signal Processing, IEE Proceedings F*, vol. 134, no. 2, pp. 174 –190, april 1987.
[13] E. Conte and M. Longo, "Characterisation of radar clutter as a spherically invariant random process," *Communications, Radar and Signal Processing, IEE Proceedings F*, vol. 134, no. 2, pp. 191 –197, april 1987.
[14] E. Jakeman and P. Pusey, "A model for non-rayleigh sea echo," *Antennas and Propagation, IEEE Transactions on*, vol. 24, no. 6, pp. 806 – 814, nov 1976.
[15] A. Farina, A. Russo, and F. Studer, "Coherent radar detection in log-normal clutter," *Communications, Radar and Signal Processing, IEE Proceedings F*, vol. 133, no. 1, pp. 39 –53, february 1986.
[16] A. Ozturk, "A general algorithm for univariate and multivariate goodness-of-fit tests based on graphical representation," *Communications in statistics - theory and methods*, vol. 20, no. 10, pp. 3111 –3137, 1991.
[17] A. Ozturk and E. Dudewicz, "A new statistical goodness-of-fit test based on graphical representation," *Biometrical Journal*, vol. 34, no. 4, pp. 403 –427, 1992.
[18] A. Ozturk, "An application of a distribution identification algorithm to signal detection problems," in *Signals, Systems and Computers, 1993. 1993 Conference Record of The Twenty-Seventh Asilomar Conference on*, nov 1993, pp. 248 –252 vol.1.
[19] P. Chen, W. Melvin, and M. Wicks, "Screening among multivariate normal data," *Journal of Multivariate Analysis*, no. 69, pp. 10 – 29, 1999.
[20] M. Rangaswamy, J. Michels, and B. Himed, "Statistical analysis of the nonhomogeneity detector for non-gaussian interference backgrounds," in *Radar Conference, 2002. Proceedings of the IEEE*, 2002, pp. 304 – 310.
[21] M. Greco, P. Stinco, F. Gini, and M. Rangaswamy, "Impact of sea clutter nonstationarity on disturbance covariance matrix estimation and cfar detector performance," *Aerospace and Electronic Systems, IEEE Transactions on*, vol. 46, no. 3, pp. 1502 –1513, july 2010.